RSC Advances

PAPER

View Article Online
View Journal | View Issue

Cite this: *RSC Adv.*, 2019, **9**, 20323

Synergistic degradation of PNP *via* coupling H_2O_2 with persulfate catalyzed by nano zero valent iron†

Jiangkun Du,[a] Yang Wang,[a] Faheem,[a] Tiantian Xu,[a] Han Zheng[b] and Jianguo Bao*[a]

H_2O_2 and persulfate (PDS) activated by iron are attracting much attention due to their strong oxidation capacity for the effective degradation of organic pollutants. However, they face problems such as requiring an acidic reaction pH and difficulty of Fe^{2+} regeneration. In this study, the simultaneous activation of H_2O_2 and persulfate by nanoscaled zero valent iron (nZVI) was investigated for the degradation of *p*-nitrophenol (PNP). The nZVI/H_2O_2/PDS oxidation system exhibited significantly higher reactivity toward PNP degradation than the systems with a single oxidant. A synergistic effect was explored between H_2O_2 and PDS during nZVI-mediated activation, and the molar ratio of H_2O_2/PDS was a key parameter in optimizing the performance of PNP degradation. The nZVI/H_2O_2/PDS system could function well in a wide pH range, and even 95% PNP was removed at an initial pH 10, thus markedly alleviating the pH limitations of Fenton-like processes. Both hydroxyl radicals and sulfate radicals could be identified during H_2O_2/PDS activation, in which H^+ produced during PDS decomposition promoted H_2O_2 activation. The increase of oxidant concentration could significantly enhance the PNP degradation, while the presence of HCO_3^- and HPO_4^{2-} exerted great inhibition. Furthermore, five degradation intermediates of PNP were detected and its degradation pathways in the nZVI/H_2O_2/PDS system were presented. This study reveals that the simultaneous activation of H_2O_2 and PDS by nZVI is a promising advanced oxidation tool as an alternative to typical Fenton processes for recalcitrant pollutant removal.

Received 17th April 2019
Accepted 10th June 2019

DOI: 10.1039/c9ra02901j

rsc.li/rsc-advances

1. Introduction

Rapid industrial development produces huge amounts of wastewater containing lots of hazardous non-biodegradable pollutants. As a widely used raw chemical material, *p*-nitrophenol (PNP) is of high toxicity and difficult to biodegrade, meaning that it can remain in the environment for a long time.[1] Untreated emissions of PNP will definitely cause water pollution and bring serious risk to the ecosystem and human health.[2] Therefore, it is crucial to develop effective techniques for rapidly and efficiently eradicating PNP present in contaminated environments. Therein, Fenton and Fenton-like processes (AOPs) have been considered as effective pathways for the degradation of a variety of hazardous and bio-refractory organics during the last decades.[3,4]

Zero valent iron (ZVI) is a well-known Fenton-like catalyst for the treatment of variety of refractory organics due to several benefits, such as cheap price and benign environmental nature.[5] Typically, ZVI can provide Fe^{2+} ions to activate H_2O_2 generating hydroxyl radicals ($\cdot OH$) through the routes presented by eqn (1)–(4). However, in case of micrometric ZVI powder applied,[6] the reactions represented by eqn (1) and (2) are slow in nature because of the low material reactivity.[7] Thus, to alleviate the limitation of ZVI/H_2O_2 system, a number of studies were carried out with incorporating additional setup such as ultrasound and heat[8,9] to speed up the electron transfer process. Besides, nano-scaled ZVI (nZVI) was also frequently studied as an alternative Fenton-like activator because of its much higher reactivity with versatile functions for contaminants removal.[10] However, no matter micro- or nano-ZVI was applied, the activation of H_2O_2 should still be initiated under acidic conditions.

$$2Fe^0 + O_2 + 2H_2O \rightarrow 2Fe^{2+} + 4OH^- \quad (1)$$

$$Fe^0 + 2H^+ \rightarrow Fe^{2+} + H_2 \quad (2)$$

$$Fe^{2+} + H_2O_2 \rightarrow Fe^{3+} + \cdot OH + OH^- \quad (3)$$

$$Fe^{3+} + H_2O_2 \rightarrow Fe^{2+} + \cdot OOH + H^+ \quad (4)$$

Alternatively, the activation of persulfate (PDS) with production of sulfate radicals ($SO_4^{\cdot -}$) has gained wide attentions in recent years. In comparison with H_2O_2-based Fenton-

[a]*School of Environmental Studies, China University of Geosciences, Wuhan 430074, People's Republic of China. E-mail: bjianguo@cug.edu.cn; Fax: +86-2-9585447; Tel: +86-2-9585426*

[b]*Hubei Provincial Key Laboratory of Mining Area Environmental Pollution Control and Remediation, Hubei Polytechnic University, Huangshi, People's Republic of China*

† Electronic supplementary information (ESI) available. See DOI: 10.1039/c9ra02901j

like processes, PDS can be effectively activated in a wide pH range as represented by eqn (5) and (6), and $SO_4^{\cdot-}$ possesses a better selectivity on pollutants oxidation. However, unlike the ZVI/H_2O_2 system that the formed Fe^{3+} can get reduced to Fe^{2+} by H_2O_2 (eqn (4)), the Fe^{3+} generated in eqn (3) is quite more stable in ZVI/PDS system, which becomes the main cause of ceasing of activation reaction as well as the generation of more iron sludge.[11,12] Recently, some studies reported the simultaneous activation of H_2O_2 and PDS, which might exert synergistic effect to alleviate the faced drawbacks as they used alone. Monteagudo *et al.* studied the activation of persulfate in assistant of UV–Fe^{2+}–H_2O_2, and found that the PDS activated by UV/Fe^{2+}/H_2O_2 presented significantly higher efficiency for carbamazepine degradation compared to other systems including PDS/Fe^{2+}, PDS/UV and H_2O_2/PDS.[13] However, without the assistant of UV irradiation, the synergistic role between H_2O_2 and PDS would be greatly hindered, as reported by Dulova *et al.*,[14,15] that traditional Fenton process showed higher efficacy for the antibiotic degradation than the combined Fe^{2+}/H_2O_2/PDS system. The possible radicals quenching might be induced by an excessive addition of ferrous ions. As an alternative, zero valent iron can act as an activator with capacity of controllable ferrous release. Li *et al.* investigated the coupling of micrometric Fe^0 with H_2O_2/PDS for the degradation of *p*-nitrophenol, and their results supported the significantly higher efficacy of the combined Fe^0/H_2O_2/PDS system than that obtained with single oxidant.[16] As concluded, the promoted iron corrosion and also alleviated Fe^0 passivation both contributed to the synergistic effect in the Fe^0/H_2O_2/PDS process. However, the effect of solution pH and the role of PDS on radical generation was not fully evaluated. Since Fenton-like reactions were pH-dependent processes, the interplay between H_2O_2 and PDS with various ratio would be remarkably affected under different pH conditions. In addition, the catalytic performance of nano-scaled ZVI for simultaneous activation of H_2O_2 and PDS is necessary to be explored given that nZVI is extensively applied for water remediation and acts very different reactive feature compared to micrometric ZVI and ferrous ions.

$$S_2O_8^{2-} + Fe^{2+} \rightarrow SO_4^{\cdot-} + Fe^{3+} + SO_4^{2-} \quad (5)$$

$$2S_2O_8^{2-} + Fe^0 \rightarrow 2SO_4^{\cdot-} + Fe^{2+} + 2SO_4^{2-} \quad (6)$$

In order to overcome the variety of limitations encountered both in nZVI/H_2O_2 and nZVI/PDS system, joint venture of nZVI/H_2O_2/PDS might be a possible solution providing synergetic degradation of organic by combining nZVI, H_2O_2 and persulfate. Furthermore, the role and catalytic mechanism of H_2O_2 and persulfate during simultaneous activation in the combined system should be further specified. Therefore, the objective of this study was to (1) explore and compare the performance evaluation of PNP degradation in nZVI/H_2O_2, nZVI/PDS, and the nZVI/H_2O_2/PDS systems; (2) to optimize key parameters involved in combined nZVI/H_2O_2/PDS process; (3) to reveal the synergistic effects existed in case of the combined nZVI/H_2O_2/PDS system; (4) to propose the possible degradation pathway of PNP as well as the mechanism involved in nZVI/H_2O_2/PDS combined system.

2. Materials and experimental procedure

2.1 Chemicals and reagents

$NaBH_4$, $FeSO_4 \cdot 7H_2O$ and *p*-nitrophenol were bought from Aladdin company. 5,5-Dimethylpyrroline-*N*-oxide (DMPO), sodium peroxydisulfate (PDS, $Na_2S_2O_8$) were supplied by Sigma-Aldrich. Methanol (MeOH) and acetic acid in HPLC-grade were obtained from Fisher Scientific, and other chemicals were provided by Sinopharm with analytical grade. All reagents were prepared by ultrapure water (18.2 MΩ cm^{-1}). The nano-scaled zero valent iron (nZVI) particles were fabricated by reducing $FeSO_4 \cdot 7H_2O$ with NaBH under nitrogen protection based on our previous report.[17]

2.2 Degradation experiments

To carry out the degradation experiments, a certain amount of PDS and H_2O_2 stock solution was spiked into *p*-nitrophenol (100 mL, 20 ppm, equal to 0.1438 mmol L^{-1}) in 250 mL glass conical flasks. The initial solution pH was adjusted using NaOH or H_2SO_4 to reach desired condition. The reactions were initiated by adding predetermined dosage of nZVI particles. The mixed reactants were stirred using a mechanical stirrer in fixed speed to maintain a good mixture. The effects of water matrices were investigated with addition of designated level of inorganic salts. At scheduled time intervals, 1 mL liquid samples were withdrawn from the reaction system, and well-mixed with 1 mL of methanol to stop the further *p*-nitrophenol oxidation initiated by reactive radicals. Then the mixed samples were immediately filtered through 0.45 μm syringe filters for HPLC measurement. To evaluate the production of hydroxyl radicals (·OH) during the reaction, benzoic acid (BA) was adopted as the substrate instead of PNP, and the generated *p*-hydroxybenzoic acid (*p*-HBA) was recorded as the ·OH indicator. As to monitor the aqueous concentration of iron ions, PDS and H_2O_2, samples were taken, filtered and analyzed immediately. Each batch test was carried out at least duplicate runs, while the average results and the standard deviations were calculated and presented in the figures.

2.3 Analytical procedures

The concentration of residual PNP was tested using RIGOL L-3000 HPLC system installed with a Compass C18 column (5 μm, 4.6 × 250 mm). Mobile phase was a mixture of methanol and 1% acetic acid at a ratio of 42 : 58 (v/v). The flow rate of mobile phase was fixed at 1.0 mL min^{-1}, and the λ_{max} of PNP was determined at 317 nm. The formed *p*-HBA was measured by HPLC at 270 nm applying a combination of 0.65% TFA and acetonitrile (65 : 35 v/v) as the mobile phase. In addition, the amounts of leached Fe ions were detected by atomic adsorption spectrometer. The concentration of H_2O_2 was analyzed at 405 nm on a spectrophotometer after chromogenic reaction with titanium sulfate.[18] The total concentration of H_2O_2/PDS in

the dual oxidants system or the concentration of PDS in single oxidant system was monitored using iodometric titration method at a detection wavelength of 350 nm because both PDS and H_2O_2 can oxidize iodide to iodine.[19] Thus the residual amount of PDS in the nZVI/H_2O_2/PDS system was quantified as the difference value between H_2O_2/PDS and H_2O_2. As to determine reactive radicals generated by interaction between nZVI and oxidants, aqueous samples were immediately withdrawn and filtered from the reaction system, mixed with DMPO, and analyzed on an EPR (JES-FA200, Hitachi) spectrometer. The identification and quantitation of the PNP intermediates were performed on an LC tandem mass spectrometry Q Exactive™ Hybrid Quadrupole-Orbitrap™ (LC-HRMS, Thermo Scientific, Bremen, Germany) equipped with an ESI (electrospray ionization) mode. The mobile phase started with 5/95 (v/v) acetonitrile/water and a flow rate of 0.2 mL min^{-1}. The mass spectra were recorded in electron-impact (EI) mode in a range of 60–750 *m*/*z* for qualitative analysis.

3. Results and discussion

3.1 Characterization of nZVI particles

The morphology of as-prepared nZVI shows that the nZVI particles have rough spherical shape and are present in chain-like aggregated form in nanoscaled size range (Fig. S1†). The XRD technique was also applied in order to evaluate the degree of crystallinity as well as the speciation for as-prepared nZVI particles. The two dominant diffraction peaks (Fig. S2†) at 2θ position of 44.68° (110) and 65.03° (200) were assigned to the typical orientation of α-Fe, supporting the higher purity and crystalline structure of nZVI particles.

3.2 Application of nZVI for catalytic degradation of PNP

As presented in Fig. 1, the PNP degradation performance in the various systems, including H_2O_2/PDS alone, nZVI alone, nZVI/PDS, nZVI/H_2O_2 and nZVI/H_2O_2/PDS, were investigated during the batch experiments. It was noticed that negligible amount of PNP was degraded when H_2O_2/persulfate were applied alone without nZVI, demonstrating the poor oxidation ability of non-activated H_2O_2 or PDS.[20] In case of nZVI alone, almost 51% of total PNP removal was noticed which was attributed to reductive capability of as-prepared nZVI nanoparticles. The nitryl group of PNP was reduced to amino with generation of *p*-aminophenol.[21] However, it was noted that the PNP removal rate achieved by nZVI alone was even higher than that obtained by nZVI/H_2O_2. A sudden removal of 24% of PNP by nZVI/H_2O_2 was observed in the first minute followed by rarely slow degradation within the rest reaction times. Since it is well-known that the activation of H_2O_2 by Fe^{2+} or Fe^0 suffers the limitation of acidic reaction condition, the initial neutral condition in the present study may not be suitable to motivate the oxidative capability of the nZVI/H_2O_2.

In comparison, relatively higher PNP degradation (83% in 60 min) was monitored in case of nZVI/PDS than nZVI/H_2O_2. This observation can be described by rapid formation of ROSs from PDS activation and sudden generation of ferric species (Fe^{3+}) as prescribed by equations scheme given by eqn (5). Similar findings were reported in literatures which confirmed the higher effectiveness of PDS than H_2O_2 during ferrous ion-activated degradation of levofloxacin.[22] On contrary, rapid and complete PNP degradation was accomplished in the reaction system combining nZVI with H_2O_2/PDS dual oxidants. These results supplied the evidence of the synergistic effect between H_2O_2 and PDS as they were activated by nZVI particles.

The residual concentration of oxidants applied during Fenton process was monitored for all nZVI/PDS, nZVI/H_2O_2 and nZVI/H_2O_2/PDS systems. As depicted in Fig. 2, significant amount of H_2O_2 was not consumed and remained in solution of the nZVI/H_2O_2 system. On the one hand, fewer of Fe^{2+} ions were produced on nZVI surface in neutral condition resulting in slower H_2O_2 decomposition mediated by ferrous.[23] On the other hand, since PNP was not effectively degraded by nZVI/H_2O_2

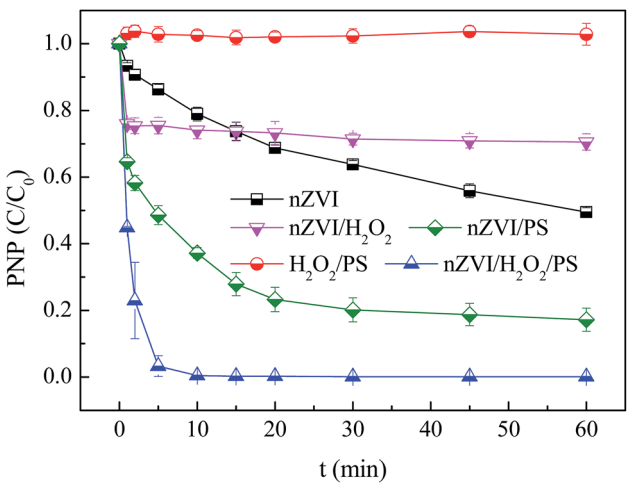

Fig. 1 Degradation of PNP in different reaction systems. Reaction condition: $[PNP]_0$ = 20 mg L^{-1}, $[H_2O_2]_0$ = 2 mmol L^{-1}, $[PDS]_0$ = 2 mmol L^{-1}, $[H_2O_2/PDS]_0$ = 2 mmol L^{-1}, $[nZVI]_0$ = 0.2 g L^{-1}, initial pH = 7. Note: in the nZVI/H_2O_2/PDS system, the molar ratio of H_2O_2/PDS was 1.

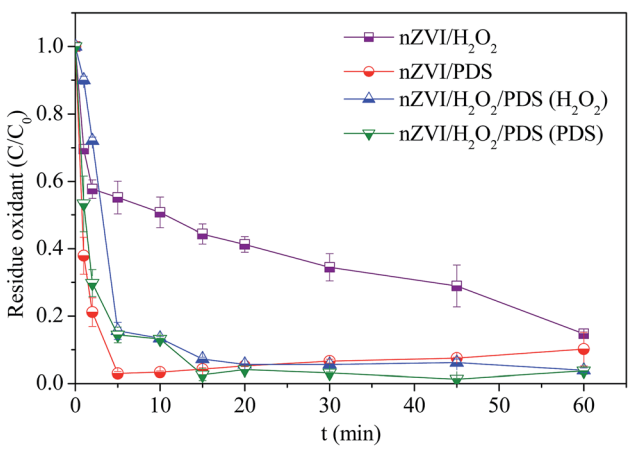

Fig. 2 Oxidants consumption in nZVI/H_2O_2, nZVI/PDS and nZVI/H_2O_2/PDS systems. Reaction condition: $[nZVI]_0$ = 0.2 g L^{-1}, $[PNP]_0$ = 20 mg L^{-1}, $[PDS]_0 = [H_2O_2]_0$ = 2 mM, $[H_2O_2/PDS\ (1:1)]_0$ = 2 mmol L^{-1}, initial pH = 7.

under the neutral conditions, H_2O_2 was only decomposed on the nZVI surface without generating reactive radical spices. In contrast, the oxidants detected in nZVI/PDS and nZVI/H_2O_2/PDS systems were consumed very fast and negligible amount of residual oxidants remained in solution after 10–15 min reaction. Additionally, it was noticed that the maximum consumption of oxidants occurred in presence of PDS which would decompose and generate H^+ protons to accelerate nZVI corrosion and in turn promote H_2O_2 activation. This confirmed that both nZVI/PDS and nZVI/H_2O_2/PDS were more applicable over nZVI/H_2O_2 Fenton-like system under neutral conditions.

In order to distinguish different radicals generated in the nZVI/H_2O_2, nZVI/PDS and nZVI/H_2O_2/PDS systems, the EPR spectra were monitored by using DMPO as spin trap during the reactions. As given in Fig. 3(a), the formation of ·OH radicals was supported by strong DMPO-OH signal in nZVI/H_2O_2 system. However, for both nZVI/PDS and nZVI/H_2O_2/PDS systems, seven peaks referred to DMPOX adduct were detected, and significantly stronger spectrum intensity was observed in the dual oxidation system. DMPOX was the final adduct obtained as a result of $SO_4^{\bullet-}$-assisted oxidation of DMPO or DMPO-OH, because DMPO/$SO_4^{\bullet-}$ was highly unstable and directly converted to DMPOX. In addition, this DMPOX pattern in the dual oxidation system was not monitored before adding nZVI catalyst (Fig. S3†), indicating the essential role of nZVI for the production of reactive radicals. The DMPOX generated and remained strong during the first several minutes, but vanished after 10 min reaction. This was consistent with the variation of oxidants concentration as shown in Fig. 2 that most of H_2O_2/PDS were consumed after 10 min reaction. The formation of DMPOX supported the involvement of $SO_4^{\bullet-}$ radicals generated as a result of PDS activation for PNP degradation route. The presence of ·OH in the nZVI/H_2O_2/PDS system was further evidenced using benzoic acid (BA) as the probe, which would transform to *p*-hydroxybenzoic acid (*p*-HBA) by reaction with ·OH. As displayed in Fig. S4,† the concentration of generated *p*-HBA increased notably along the time profile, implying the significant production of ·OH during simultaneous H_2O_2/PDS activation.

To further ensure the role of ·OH and $SO_4^{\bullet-}$ towards PNP degradation, quenching tests with chemical probes were further performed. In specific, *tert*-butyl alcohol (TBA) without α-hydrogen was added as a scavenger for ·OH radicals due to its tendency to react faster with ·OH than $SO_4^{\bullet-}$ radicals. In addition, methanol (MeOH) with α-hydrogen is commonly utilized as a quenching reagent for both $SO_4^{\bullet-}$ and ·OH radicals. As shown in Fig. 3(b), the great decrease in PNP degradation was noticed when 1000 mmol L^{-1} alcohols (alcohol : PDS = 500 : 1) were added into the nZVI/H_2O_2/PDS system. MeOH exhibited a slightly higher inhibition rate on PNP degradation compared to TBA, indicating that both $SO_4^{\bullet-}$ and ·OH were predominant radicals in the nZVI/H_2O_2/PDS system.

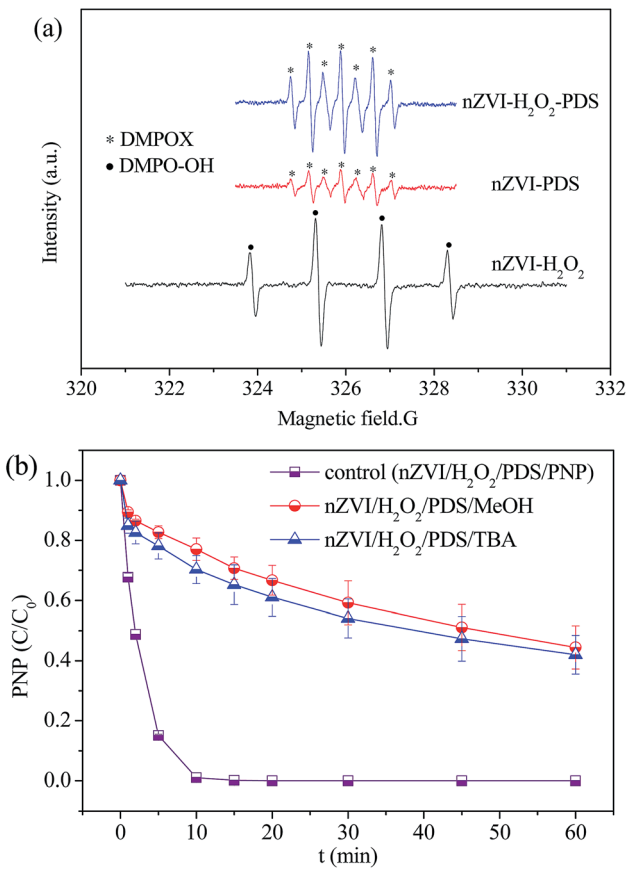

Fig. 3 (a) EPR spectra obtained for nZVI/H_2O_2, nZVI/PDS and nZVI/PDS/H_2O_2 systems; (b) degradation of PNP in the nZVI/PDS/H_2O_2 system with addition of MeOH and TBA. Reaction condition: $[nZVI]_0$ = 0.2 g L^{-1}, $[PNP]_0$ = 20 mg L^{-1}, $[PDS]_0 = [H_2O_2]_0$ = 2 mM, $[H_2O_2/PDS\ (1:1)]_0$ = 2 mmol L^{-1}, $[MeOH\ or\ TBA]_0$ = 1000 mmol L^{-1}.

3.3 Effect of pH

The effect of initial pH on the removal efficiency of PNP was investigated based on different reaction systems, including nZVI/H_2O_2, nZVI/PDS and nZVI/H_2O_2/PDS with different molar ratio between H_2O_2 and PDS. As shown in Fig. 4, the pH range of 3–10 was adopted to evaluate the performance for all Fenton-like systems. The system of nZVI/H_2O_2 exhibited an extremely high efficiency for PNP degradation at initial pH 3 that complete PNP removal was achieved within 5 min reaction. However, its performance at pH 5, pH 7 and pH 10 was unsatisfied due to its intrinsic pH limitation.[24] On contrary, the PNP degradation by nZVI/PDS was slightly affected by the initial solution pH. Overall 80% of PNP could be removed within 60 min reaction in the nZVI/PDS system while changing initial pH from 3 to 10. These results were consistent with some early studies that persulfate oxidation of PNP was not sensitive to the variation of solution pH.[25,26] According to the above results, nZVI/H_2O_2 possessed a stronger oxidation ability towards PNP than that obtained by nZVI/PDS under optimized pH conditions (pH = 3). This might be due to the generation of different ROSs from nZVI/H_2O_2 and nZVI/PDS, resulting in dissimilar reactivity to PNP compound. For the combined system of nZVI/H_2O_2/PDS, PNP could be rapidly and completely degraded within the first 10 min in both acidic and neutral conditions, while this process became significantly slower in alkaline environment at pH 10. In addition, the maximum PNP removal was noticed when 1 : 1 ratio of

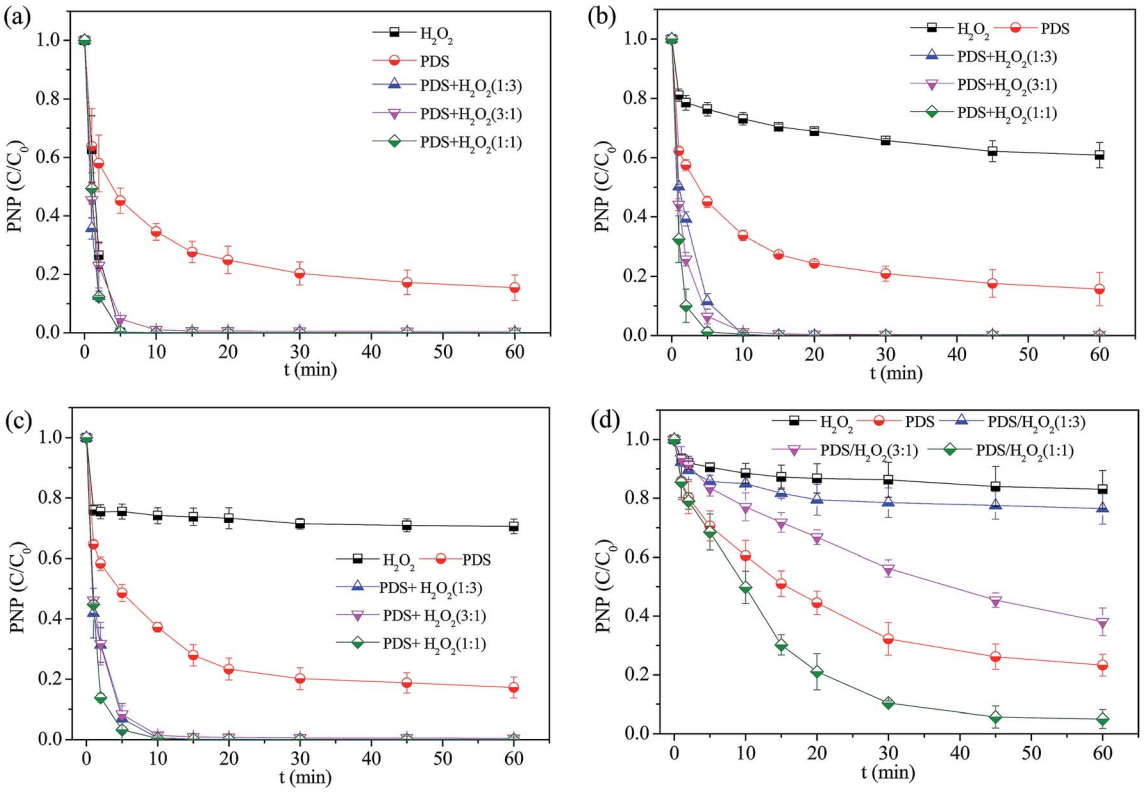

Fig. 4 PNP degradation in different oxidation systems with different initial pH (a) pH = 3, (b) pH = 5, (c) pH = 7, (d) pH = 10. Reaction condition: $[nZVI]_0 = 0.2$ g L^{-1}, $[PNP]_0 = 20$ mg L^{-1}, $[H_2O_2]_0 = 2$ mmol L^{-1}, $[PDS]_0 = 2$ mmol L^{-1}, $[H_2O_2/PDS]_0 = 2$ mmol L^{-1}.

H_2O_2–PDS was employed than others H_2O_2–PDS ratios such as 1 : 3 and 3 : 1 when different oxidants ratios were adopted. These results indicated that the simultaneous activation of H_2O_2 and PDS by nZVI exhibited better application potential for pH variation and synergistic effect on PNP degradation compared to the systems with single oxidant.

Table 1 presents the value of solution pH before and after the reactions. It was noted that the pH value kept stable for the system of nZVI/H_2O_2, but decreased remarkably to the range of 3–4 for the system of nZVI/PDS no matter the initial pH was 3 or 10. This pH transformation was likely to promote the H_2O_2-based Fenton-like degradation of PNP in the nZVI/H_2O_2/PDS dual oxidants system. In neutral or alkaline conditions, PDS would be first activated by nZVI along with the decrease of solution pH to 3–4 at which H_2O_2 activation was sequentially initiated for further PNP oxidation. Therefore, the optimum ratio between H_2O_2 and PDS was a key parameter for PNP degradation in view of efficiency, economy as well as environmental safety point since replacement of PDS by H_2O_2 would reduce SO_4^{2-} discharge to receiving water bodies.

The activation of H_2O_2 and persulfate on nZVI would also result in iron release in some extent. Thus the release of Fe ions from nZVI in different reaction systems at initial pH 7 was further investigated. As depicted in Fig. 5, less Fe ions were released in the ZVI/H_2O_2 system, while over 90 mg L^{-1} Fe irons escaped in the ZVI/PDS system. The acidic nature of PDS would promote iron corrosion and lead to high Fe ions release. For the systems with dual oxidants, as high as 71.8 mg L^{-1} aqueous Fe ions were detected in terms of higher PDS proportion (PDS : H_2O_2 = 3 : 1), but about 20 mg L^{-1} Fe ions released as the PDS/H_2O_2 ratios was 1 : 1 and 1 : 3. This was attributed to fast conversion of generated Fe^{3+} into Fe^{2+} in the presence of H_2O_2. In fact, the formation of inactive iron species including ferric ions as well as oxyhydroxides not only lead to nZVI passivation but also result in scavenge of the formed ·OH and $SO_4^{\cdot-}$. However, the introduction of H_2O_2 into PDS-based oxidation systems could alleviate this drawback to some extent. As a summary, for all pH values including pH 3, the combination of H_2O_2 with PDS system depicted higher PNP removal than nZVI/H_2O_2 and nZVI/PDS systems, confirming the synergistic effect of the dual oxidant due to more feasible pH variation and iron release.

3.4 Effect of oxidant dosage

In order to investigate the effect of combined use of oxidants H_2O_2 and PDS for the degradation of PNP, the different dosages of dual oxidants were taken from 0.5 mM to 1.0 mM by keeping the ratio constant at 1 : 1. It was noticed that the increase of H_2O_2/PDS dosage accelerated the degradation of PNP, and complete PNP removal could be observed as the total H_2O_2/PDS concentration increased over than 1.5 mM (Fig. 6). Even though it was reported that H_2O_2 was able to enhance PDS oxidation of pollutants, in which the combined persulfate/H_2O_2 based advanced oxidation process was implemented for the treatment

Table 1 Results summarized for PNP degradation at different initial pH in various reaction systems[a]

Reaction systems	H_2O_2 concentration (mmol L^{-1})	PDS concentration (mmol L^{-1})	pH (average value)		Removal rate of PNP
			Initial	Final	
nZVI/H_2O_2	2.0	—	3.0	4.9	100%
nZVI/PDS	—	2.0	3.0	3.22	84.5%
nZVI/H_2O_2/PDS (3 : 1)	1.5	0.5	3.0	3.89	100%
nZVI/H_2O_2/PDS (1 : 1)	1.0	1.0	3.0	3.74	100%
nZVI/H_2O_2/PDS (1 : 3)	0.5	1.5	3.0	3.48	99.5%
nZVI/H_2O_2	2.0	—	5.07	6.38	39.1%
nZVI/PDS	—	2.0	5.07	3.17	84.3%
nZVI/H_2O_2/PDS (3 : 1)	1.5	0.5	5.07	3.97	100%
nZVI/H_2O_2/PDS (1 : 1)	1.0	1.0	5.07	3.43	100%
nZVI/H_2O_2/PDS (1 : 3)	0.5	1.5	5.07	3.24	99.6%
nZVI/H_2O_2	2.0	—	7.01	6.94	29.4%
nZVI/PDS	—	2.0	7.01	2.88	82.8%
nZVI/H_2O_2/PDS (3 : 1)	1.5	0.5	7.01	4.44	100%
nZVI/H_2O_2/PDS (1 : 1)	1.0	1.0	7.01	3.59	100%
nZVI/H_2O_2/PDS (1 : 3)	0.5	1.5	7.01	3.02	99.9%
nZVI/H_2O_2	2.0	—	9.96	8.47	16.9%
nZVI/PDS	—	2.0	9.96	3.34	76.7%
nZVI/H_2O_2/PDS (3 : 1)	1.5	0.5	9.96	6.1	23.5%
nZVI/H_2O_2/PDS (1 : 1)	1.0	1.0	9.96	3.45	94.9%
nZVI/H_2O_2/PDS (1 : 3)	0.5	1.5	9.96	3.52	61.9%

[a] The initial concentration of nZVI and PNP was 0.2 g L^{-1} and 20 mg L^{-1} (equal to 0.1438 mmol L^{-1}), respectively.

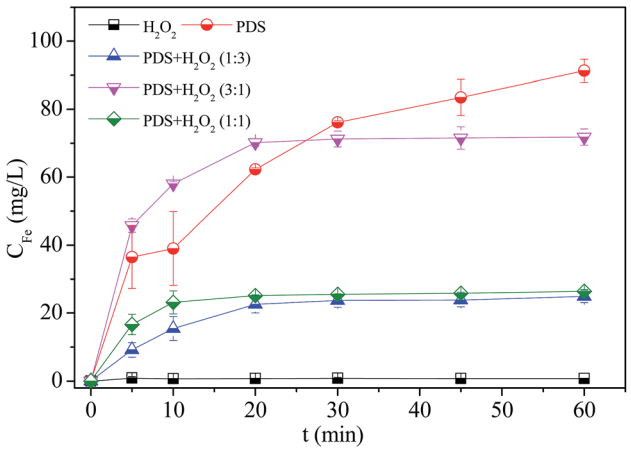

Fig. 5 Concentration of leached iron in nZVI/H_2O_2, nZVI/PDS and nZVI/H_2O_2/PDS systems. Reaction condition: $[nZVI]_0$ = 0.2 g L^{-1}, $[PNP]_0$ = 20 mg L^{-1}, $[H_2O_2]_0$ = $[PDS]_0$ = 2 mM, $[H_2O_2/PDS\ (1:1)]_0$ = 2 mmol L^{-1}, initial pH = 7.

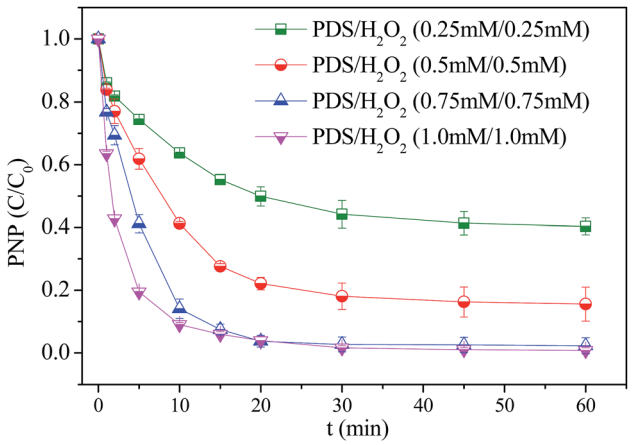

Fig. 6 PNP degradation in the nZVI/H_2O_2/PDS system with different oxidant dosage. Reaction condition: $[nZVI]_0$ = 0.2 g L^{-1}, $[PNP]_0$ = 20 mg L^{-1}, $[H_2O_2]_0/[PDS]_0$ = 1 : 1, initial pH = 7.

of landfill leachate.[27] However, the PDS/H_2O_2 couple hardly degraded PNP in the present study. Therefore, the increase of oxidants induce more ROSs for PNP degradation because more PDS/H_2O_2 was catalytically activated on nZVI.

In comparison, different performances of nZVI/H_2O_2 and ZVI/PDS oxidation systems were observed with increasing oxidant dosage (Fig. S5†). Because of unavailable activation of H_2O_2 in neutral conditions, no improvement but decrease in PNP was monitored with the increase of H_2O_2 dosage in nZVI/H_2O_2 Fenton-like system. The maximum PNP removal was achieved when the H_2O_2 concentration was 0.5 mM. For the system of nZVI/PDS, the degradation of PNP was enhanced when the PDS dosage increased from 0.5 mM to 1.0 mM, but remained similar as further increase to 1.5 mM and 2.0 mM. It could be due to the limited ferrous and Fe^0 active site to generate optimized or enough $SO_4^{\bullet-}$ which boost up the PNP removal to some extent.

3.5 Effect of water matrices

The effect of inorganic ions normally available in real wastewater on PNP removal performance was investigated. The Cl^-, HCO_3^-, NO_3^-, HPO_4^{2-} anions which were considered as most common water matrices were selected as probe ions. The

experimental evidences revealed that HCO_3^- and HPO_4^{2-} anions were dominant water matrix affecting the PNP removal performance when compared with others anions encountered at optimized pH value 7. As shown in Fig. 7, unobvious change was noticed for PNP removal with the addition of Cl^- ions, indicating that Cl^- could not quench ·OH and $SO_4^{\cdot-}$ species. Moreover, the slight decrease in PNP degradation was examined when NO_3^- was incorporated in the nZVI/H_2O_2/PDS dual oxidation system. Since NO_3^- ions was unable to form complexes with Fe^{2+}/Fe^{3+} and also showed non-reactive nature for ·OH radicals.[28] This phenomenon could be assigned to the scavenging effect of NO_3^- on $SO_4^{\cdot-}$ species given that they could react at a rate of 5.0×10^4 M^{-1} S^{-1}.[29,30] In case of HCO_3^-, the profound inhibitory effect on PNP removal efficiency was monitored. This was attributed to scavenging reaction between ·OH/$SO_4^{\cdot-}$ and HCO_3^-, and also the nZVI passivation caused by precipitation with Fe^{2+}/Fe^{3+}. Similarly, for HPO_4^{2-} ions the remarkable inhibitory effect on PNP degradation was depicted because HPO_4^{2-} could complex with reactive Fe^{2+}, therefore, competing the interaction with H_2O_2/PDS oxidants.[31]

3.6 Degradation pathways of PNP

Six intermediates were identified by LC-HRMS and their molecular structures were preliminarily speculated to further analyze the pathway of PNP decomposition. It can be seen from Table S1 and Fig. S6† that five corresponding byproducts were captured from the PNP oxidation *via* nZVI catalyzed H_2O_2/PDS. Fumaric acid, oxalic acid, 5-nitro-1,2,3-benzenetriol, *p*-nitrosophenol, 4-nitrocatechol, and 2,4-dinitrophenol were detected at the residence time of 2.02 min, 2.14 min, 3.70 min, 4.50 min and 8.33 min, respectively. Based on the above intermediates, the possible pathways of PNP degradation in the nZVI/H_2O_2/PDS system were proposed in Fig. 8. Firstly, hydroxyl radicals and sulfate radicals preferred to attack the nitro substituent on the benzene ring on account of high reaction rate and non-selectivity. It was postulated that PNP was denitrated with the production of phenol. However, phenol was not detected in the product, probably because the oxidation reaction was so fast that the formed phenols immediately attacked by residual free radicals in the system and converted to other products. Denitration reaction was accompanied by the generation of a large amount of nitro radicals, which further attacked the meta position of hydroxyl radicals on the benzene ring to form 2,4-dinitrophenol.[32,33] Secondly, in view of the strong electron-pushing ability and also the electrophilicity of hydroxyl radicals, it was more likely to undergo an additional hydroxylation reaction at the meta-position of the benzene ring, thereby producing 4-nitrocatechol. In addition, 4-nitrocatechol could further undergo electrophilic oxidation to form 5-nitro-1,2,3-benzenetriol. Furthermore, because of the strong reducing ability of nZVI, a part of the PNP in the reaction system could also be directly reduced on nZVI to form *p*-nitrosophenol. Finally, benzene rings of intermediates were opened and then oxidized to form small molecular organic acids, such as fumaric acid and oxalic acid, and finally mineralized into CO_2 and H_2O.

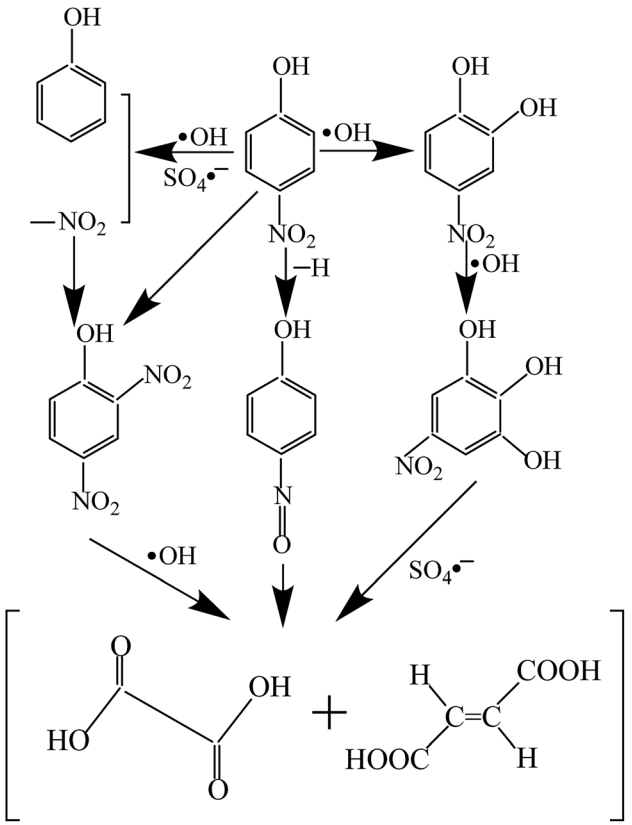

Fig. 8 Possible reaction pathways of PNP degradation in the nZVI/H_2O_2/PDS dual oxidation system.

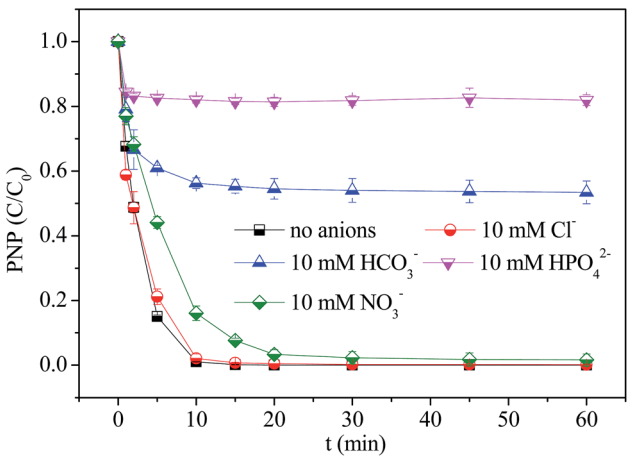

Fig. 7 The effect of water matrices on PNP degradation in the nZVI/H_2O_2/PDS system. Reaction condition: $[nZVI]_0 = 0.2$ g L^{-1}, $[PNP]_0 = 20$ mg L^{-1}, $[H_2O_2/PDS\ (1:1)]_0 = 2$ mM.

3.7 Implications of the synergistic effect between H_2O_2 and PDS

The instructive implications of the present study will be beneficial for the improvement and optimization of typical H_2O_2-based or PDS-based advanced oxidation processes as elucidated in Fig. 9. As for the nZVI/H_2O_2 Fenton-like reaction, the oxidative degradation of recalcitrant pollutants by ·OH should be

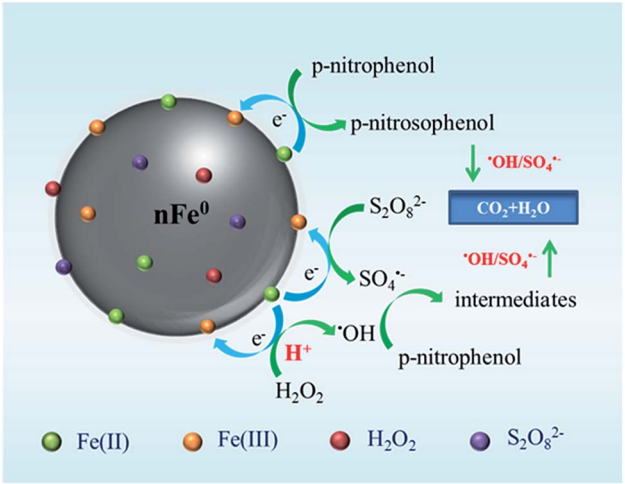

Fig. 9 Proposed mechanisms for simultaneous activation of H_2O_2/PDS with nZVI as the activator.

typically carried out in narrow pH conditions,[34] especially at pH 3. The reaction between nZVI and H_2O_2 under improper pH condition would result in invalid H_2O_2 decomposition. In contrast, the activation of PDS by nZVI with generation of $SO_4^{\cdot-}$ could be conducted in a wide pH range, but producing too much H^+ protons thus remarkably decrease the solution pH. Therefore, their distinct features comprised H_2O_2 and PDS as a complementary group.

At pH 3, both H_2O_2 and PDS could be easily activated by nZVI in the nZVI/H_2O_2/PDS system for the degradation of PNP. However, in neutral or alkaline conditions, nZVI/H_2O_2 could hardly run so that only PDS was activated during the initial stage. The H^+ protons produced from catalytic PDS activation would decrease solution pH to acidic condition (pH 3–4) and facilitate further activation of H_2O_2 with ·OH formation. Meanwhile, the corrosion of nZVI induced by PDS oxidation was accompanied by the concomitant production of a mass of Fe^{3+}. However, significant amount of these Fe^{3+} could be reduced to Fe^{2+} by H_2O_2 as evidenced in Fig. 5, in turn promoted the PDS or H_2O_2 activation.[14]

In addition, even though both ·OH and $SO_4^{\cdot-}$ possess high oxidizing capacity, $SO_4^{\cdot-}$ is more likely to degrade organic pollutants *via* electron transfer while ·OH prefers to nucleophilic attack by hydroxylation and H abstraction. For example, the degradation of PNP by ·OH mainly generated intermediates including hydroquinone, benzoquinone and multi-hydroxy benzene as reported previously.[3] However, it was demonstrated that the processes of denitration and renitration were more frequently occurred during the $SO_4^{\cdot-}$-mediated degradation of nitrobenzene.[35] Therefore, the coexistence of comparable amount of $SO_4^{\cdot-}$ and ·OH from the simultaneous activation of H_2O_2 and PDS would initiate a multi-radical attack and resulted in a more efficient or complete PNP degradation.

4. Conclusion

This study investigated the simultaneous activation of H_2O_2 and PDS using nZVI as the activator for the degradation of PNP. Compared to nZVI, nZVI/H_2O_2 and nZVI/PDS systems, the nZVI/H_2O_2/PDS oxidation system exhibited significantly higher efficiency towards PNP degradation proving the synergistic effect between H_2O_2 and PDS. Effect of pH on PNP degradation indicated that the nZVI/H_2O_2 process could only successfully run at pH 3, while the nZVI/PDS system was not sensitive to pH variation. Conversely, the join of PDS accelerated the activation of H_2O_2 by producing H^+, and enable the nZVI/H_2O_2/PDS system to proceed efficient in a wide initial pH range from 3 to 10. The best performance of nZVI/H_2O_2/PDS was achieved when the H_2O_2/PDS molar ratio was 1 : 1, and even 95% of PNP could be degraded within 60 min reaction even at pH 10. It was depicted that the activation of PDS would decrease solution pH and alleviate nZVI passivation, thus creating a favorable condition for subsequent H_2O_2 activation.

Water anions were significant interferential factors for the nZVI/H_2O_2/PDS system. The presence of carbonate and phosphate anions would remarkably inhibit PNP degradation and nitrate would exert slight inhibition. The EPR characterization and quenching tests suggested that both $SO_4^{\cdot-}$ and ·OH played dominant role for the degradation of PNP. The identified intermediates behind PNP degradation in the nZVI/H_2O_2/PDS system suggested that nitro-reduction by nZVI, hydroxylation and denitration induced by radicals oxidation were main transformation routes. As a summary, the proposed nZVI/H_2O_2/PDS synergistic system should serve as an improved and efficient Fenton-like process with multi-radicals generation for recalcitrant organic pollutants removal.

Conflicts of interest

There are no conflicts to declare.

Acknowledgements

The study was supported by the Natural Science Foundation of Hubei Province (2018CFB262), Fundamental Research Funds for the Central Universities of the China University of Geosciences (Wuhan) (No. CUG170646) and the Open Funds of Hubei Key Laboratory for Mine Environmental Pollution Control and Remediation (2014103).

References

1 S. A. Dos, M. F. Viante, D. J. Pochapski, A. J. Downs and A. Cap, *J. Hazard. Mater.*, 2018, **355**, 136–144.
2 Z. I. Bhatti, H. Toda and K. Furukawa, *Water Res.*, 2002, **36**, 1135–1142.
3 M. A. Oturan, J. Peiroten, P. Chartrin and A. J. Acher, *Environ. Sci. Technol.*, 2000, **34**, 3474–3479.
4 A. Mirzaei, Z. Chen, F. Haghighat and L. Yerushalmi, *Chemosphere*, 2017, **174**, 665–688.
5 X. Guan, Y. Sun, H. Qin, J. Li, I. M. Lo, D. He and H. Dong, *Water Res.*, 2015, **75**, 224–248.
6 L. Xu and J. Wang, *J. Hazard. Mater.*, 2011, **186**, 256–264.
7 D. H. Bremner, A. E. Burgess, D. Houllemare and K.-C. Namkung, *Appl. Catal., B*, 2006, **63**, 15–19.

8 N. Zhang, G. Xian, X. Li, P. Zhang, G. Zhang and J. Zhu, *Front. Chem.*, 2018, **6**, 12.
9 N. Liu, F. Ding, C.-H. Weng, C.-C. Hwang and Y.-T. Lin, *J. Environ. Manage.*, 2018, **206**, 565–576.
10 W. Wang, M. Zhou, Q. Mao, J. Yue and X. Wang, *Catal. Commun.*, 2010, **11**, 937–941.
11 C. Liang, C.-P. Liang and C.-C. Chen, *J. Contam. Hydrol.*, 2009, **106**, 173–182.
12 G. P. Anipsitakis and D. D. Dionysiou, *Environ. Sci. Technol.*, 2004, **38**, 3705–3712.
13 J. M. Monteagudo, A. Durán, R. González and A. J. Expósito, *Appl. Catal., B*, 2015, **176–177**, 120–129.
14 I. Epold, M. Trapido and N. Dulova, *Chem. Eng. J.*, 2015, **279**, 452–462.
15 N. Dulova, E. Kattel and M. Trapido, *Chem. Eng. J.*, 2017, **318**, 254–263.
16 J. Li, Q. Ji, B. Lai and D. Yuan, *J. Taiwan Inst. Chem. Eng.*, 2017, **80**, 686–694.
17 J. Du, J. Bao, C. Lu and D. Werner, *Water Res.*, 2016, **102**, 73–81.
18 G. M. Eisenberg, *Ind. Eng. Chem., Anal. Ed.*, 1943, **15**, 327–328.
19 C. Liang, C.-F. Huang, N. Mohanty and R. M. Kurakalva, *Chemosphere*, 2008, **73**, 1540–1543.
20 T. Olmez-Hanci, I. Arslan-Alaton and B. Genc, *J. Hazard. Mater.*, 2013, **263**(part 2), 283–290.
21 Y. Ren, J. Li, L. Lai and B. Lai, *Chemosphere*, 2018, **194**, 634–643.
22 I. Epold and N. Dulova, *J. Environ. Chem. Eng.*, 2015, **3**, 1207–1214.
23 J. Liu, C. Ou, W. Han, J. Shen, H. Bi, X. Sun, J. Li and L. Wang, *RSC Adv.*, 2015, **5**, 57444–57452.
24 J. Du, W. Guo, D. Che and N. Ren, *Chem. Eng. J.*, 2018, **351**, 532–539.
25 J. Li, Y. Ren, F. Ji and B. Lai, *Chem. Eng. J.*, 2017, **324**, 63–73.
26 X. Chen, M. Murugananthan and Y. Zhang, *Chem. Eng. J.*, 2016, **283**, 1357–1365.
27 A. H. Hilles, S. S. A. Amr, R. A. Hussein, O. D. El-Sebaie and A. I. Arafa, *J. Environ. Manage.*, 2016, **166**, 493–498.
28 J. De Laat, G. T. Le and B. Legube, *Chemosphere*, 2004, **55**, 715–723.
29 T. Umschlag, R. Zellner and H. Herrmann, *Phys. Chem. Chem. Phys.*, 2002, **4**, 2975–2982.
30 Y. Xu, Z. Lin and H. Zhang, *Chem. Eng. J.*, 2016, **285**, 392–401.
31 D. Whebi, H. Hafez, M. El Masri and M. El Jamal, *J. Univ. Chem. Technol. Metall.*, 2010, **45**, 303–312.
32 C. Cheng, Y. Han, G. Jing, L. Zhou and Y. Lan, *J. Taiwan Inst. Chem. Eng.*, 2018, **88**, 169–176.
33 Z. Mi, X. Chen, Z. He, M. Murugananthan and Y. Zhang, *Chem. Eng. J.*, 2015, **264**, 39–47.
34 J. Deng, H. Dong, C. Zhang, Z. Jiang, Y. Cheng, K. Hou, L. Zhang and C. Fan, *Sep. Purif. Technol.*, 2018, **202**, 130–137.
35 Y. Ji, Y. Shi, L. Wang and J. Lu, *Chem. Eng. J.*, 2017, **315**, 591–597.